

# Cellulose Microfibrils from Potato Tuber Cells: Processing and Characterization of Starch–Cellulose Microfibril Composites

ALAIN DUFRESNE, DANIELE DUPEYRE, MICHEL R. VIGNON

Centre de Recherches sur les Macromolécules Végétales (CERMAV–CNRS), Université Joseph Fourier, BP 53, F-38041 Grenoble cedex 9, France

Received 7 July 1999; accepted 11 October 1999

**ABSTRACT:** The ultrastructure and morphology of potato (*Solanum tuberosum L.*) tuber cells were investigated by optical, scanning, and transmission electron microscopies. After removal of starch granules, pectins and hemicelluloses were solubilized under alkaline conditions. The alkaline insoluble residue consisted mainly of primary cell wall cellulose, which can be disintegrated under shearing to produce a homogenized microfibril suspension, as reported in a previous work.<sup>40</sup> Composite materials were processed from this potato cellulose microfibril suspension, gelatinized potato starch as a matrix and glycerol as a plasticizer. After blending and casting, films were obtained by water evaporation. The mechanical properties and water absorption behavior of the resulting films were investigated, and differences were observed depending on the glycerol, cellulose microfibrils, and relative humidity content. © 2000 John Wiley & Sons, Inc. *J Appl Polym Sci* 76: 2080–2092, 2000

**Key words:** potato tuber cells; starch; cellulose microfibrils; composite; mechanical properties; water absorption

## INTRODUCTION

There is currently a wide revival of interest in the use of biopolymers for applications in which synthetic polymers have traditionally been the materials of choice. For instance, the processing of biodegradable packaging materials containing renewable raw materials is a current research topic. In this way, there has been considerable attention during the past two decades to the utilization of gelatinized starch for single-use biodegradable plastic items such as trash bags, shopping bags, diner utensils, planting pots, and diapers.<sup>1–7</sup> The potential advantages of such materials are their established biodegradability and that they may

be disposed of by microbial action in compost piles or at sea rather than accumulating in landfills and waterways.<sup>8–10</sup> In addition to these environmental advantages, starch, or any product from agricultural sources, is of interest because of its low cost and its availability as a renewable resource. Moreover, the use of starch in plastic materials would reduce dependence on synthetic polymers made from imported oil and offers socioeconomic benefits because it generates rural jobs and a nonfood agricultural-based economy.

In fact, starch is not truly a thermoplastic as are most synthetic polymers. However, it can be melted with the addition of water and made to flow at high temperatures under pressure and shear. If the mechanical shear becomes too high, then starch will degrade to form products with low molecular weight. This results from the glass transition temperature ( $T_g$ ) and melting temper-

Correspondence to: A. Dufresne (dufresne@cermav.cnrs.fr).

*Journal of Applied Polymer Science*, Vol. 76, 2080–2092 (2000)  
© 2000 John Wiley & Sons, Inc.

ature ( $T_m$ ) of pure dry starch, which have been estimated to be 230°C<sup>11</sup> and 220–240°C,<sup>12</sup> respectively. These temperatures are higher than the temperature at which starch begins to decompose (about 220°C).<sup>13</sup> In order to extrude or mold an object from starch, it should be converted into a thermoplastic starch (TPS). The addition of water or other plasticizers (generally polyols, such as glycerol) enables starch to flow under milder conditions and considerably reduces degradation.<sup>14–17</sup> Afterwards it can be shaped into single-use biodegradable molded articles using standard thermoplastic-processing techniques, such as extrusion, injection molding, or compression molding.

By itself, starch is a poor choice as a replacement for any plastic. It is mostly water soluble, difficult to process, and brittle when used without the addition of a plasticizer. In addition, its mechanical properties are very sensitive to moisture content, which is difficult to control. In principle, some properties of starch can be significantly improved by blending it with synthetic polymers. The physical incorporation of granular starch or starch derivatives as functional additive and filler into synthetic polymers during processing has been the usual method since the first announcements of using starch in combination with synthetic polymer, either as starch–gel blends with ethylene/acrylic acid copolymers by Westhoff et al.<sup>18</sup> or as particulate starch dispersions in polyolefines by Griffin.<sup>19</sup> However, the mechanical properties of films are generally reduced by incorporation of starch. Like most polymers, starch is immiscible with most synthetic polymers at the molecular level. Another way of using starch in the material field is the processing of starch microcrystals, which can be obtained as an aqueous suspension. This filler can be dispersed in a polymeric matrix, and it has been shown to bring a great reinforcing effect.<sup>20,21</sup>

Yet these materials are not biodegradable, and thus the advantage of using a biodegradable polysaccharide is lost. In this respect, a natural fiber such as cellulose, which is biodegradable, would be a much better choice as a filler for starch. The use of natural polysaccharides as fillers and reinforcements in thermoplastics has been gaining acceptance in commodity plastics applications for many years. Most prior research on polysaccharide fillers for use in the plastics industry dealt with the use of low-cost particulate flour, such as wood, shell, and stone fruit flours.<sup>22,23</sup> Enhanced properties can be obtained by using natural cel-

lulosic fibers, such as sisal,<sup>24,25</sup> cotton,<sup>26</sup> bamboo,<sup>27</sup> jute,<sup>28</sup> straw,<sup>29</sup> kenaf,<sup>30</sup> and wood.<sup>31,32</sup> Compared to inorganic fillers, composites based on lignocellulosic fibers offer a number of benefits. These include: a renewable nature, a wide variety of fillers available throughout the world, low energy consumption, low cost, low density, high specific strength and modulus (desirable fiber aspect ratio), high sound attenuation, comparatively easy processability due to their flexibility and nonabrasive nature (which allow high filling levels, resulting in significant cost savings), and a relatively reactive surface (which can be used for grafting specific groups).

Nevertheless, despite these attractive properties, lignocellulosic fillers are used only to a limited extent in industrial practices, mainly due to difficulties associated with surface interactions. The inherent polar and hydrophilic nature of cellulose and the nonpolar characteristics of most thermoplastics result in difficulties in compounding the filler and the matrix, and therefore in achieving acceptable dispersion levels, which usually lead to poor performance composites. This hydrogen bonding is best exemplified in paper where these secondary interactions provide the basis of its mechanical strength.

An alternative way to palliate this restriction consists of obtaining both components (matrix and filler) dispersed in water. Previous works performed in our laboratory dealt with the preparation of colloidal suspensions of either cellulose whiskers or starch microcrystals.<sup>20,21,33–36</sup> Cellulose can also be used as a microfibrillar filler, which is more accessible in terms of available amounts and preparation. They consist of cellulose molecules stabilized laterally by hydrogen bonds between hydroxyl groups of adjacent molecules. Cellulose microfibrils can be found as intertwined microfibrils in the parenchyma cell wall, in particular from the sugar beet<sup>37–39</sup> or from potato pulp.<sup>40</sup> They can be extracted from the biomass by a chemical treatment leading to purified cellulose, followed by a mechanical treatment in order to obtain a homogeneous suspension due to the individualization of the microfibrils.<sup>40,41</sup>

Polysaccharide-filler aqueous suspensions can be used afterward to process composite materials with a high level of dispersion by mixing then with a latex or a water-soluble polymer as the matrix.<sup>20,21,33–36</sup> In a previous work<sup>41</sup> composite materials were obtained from a potato pulp cellulose microfibril suspension and an aqueous suspension of gelatinized potato starch as the matrix.

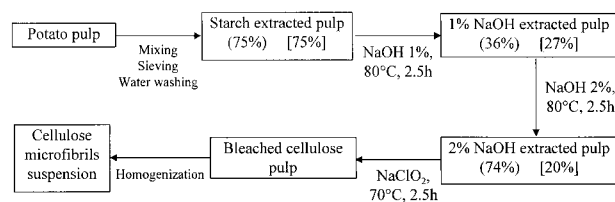


**Figure 1** Chemical and mechanical treatments of potato pulp. Data into brackets correspond to the yield of insoluble residue recovered at each step, and data into square brackets refer to the cumulative yield from starting material.

Improved thermomechanical properties and a decrease of the water sensitivity of these systems were reported.<sup>40</sup> In the present study the high-strain tensile behavior and water sorption behavior of such systems is analyzed as a function of glycerol, cellulose microfibrils, and relative humidity content.

## EXPERIMENTAL

### General Methods

Uronic acid was determined according to the method of Blumenkrantz and Asboe-Hansen.<sup>42</sup> The neutral sugars were identified and quantified by GLC of the corresponding alditol acetates,<sup>43</sup> using a Packard and Becker 417 instrument coupled to a Hewlett-Packard 3380A integrator. Glass columns (3 mm × 2 m) packed with 3% SP 2340 on Chromosorb W-AW DMCS (100–120 mesh), or 3% OV 17 on the same support, were used.

### Materials

Potato tubers can be used to produce potato starch. After removal of starch granules, the remaining pulp is traditionally pressed and dried to be marketed as cattle feed. This by-product was provided as pellets by Avebe Company (Haussimont, France). It contains around 40% cellulose, as well as the remaining starch, pectins, hemicelluloses and lignin.

### Purification of Cellulose Microfibrils

Potato pulp was purified according to the treatment reported in Figure 1 and described elsewhere.<sup>40</sup> The pellets were first hydrated into water and ground in a Waring blender apparatus for 10 min at a water-to-pulp ratio of 20 to 1. The

potato slurry was then poured on a 0.25-mm sieve and washed with water to remove small particles and the remaining starch granules. The insoluble residue was then extracted twice with a 2% sodium hydroxide solution at 80°C for 2.5 h to give an insoluble residue that was founded at around 26–28% of the starting material. After a bleaching treatment with a sodium chlorite (NaClO<sub>2</sub>) solution in a buffer medium (sodium acetate buffer, pH = 4.9) for 2.5 h at 70°C, and according to Wise et al.,<sup>44</sup> the cellulose residue was washed extensively with distilled water and freeze-dried. The purified parenchyma cell cellulose (PCC) was suspended in distilled water (2 wt %) and disintegrated for 15 min in a Waring blender. The suspension was then homogenized by 15 passes through a Manton Gaulin laboratory homogenizer (APV France, Evreux, France),<sup>45</sup> operated at 500 bars and at a temperature that was controlled at 90–95°C, as already described by Dinand et al.<sup>37,38</sup>

### Film Processing

Composite materials were processed from potato cellulose microfibrils, with potato starch as the matrix and glycerol as the plasticizer. The cellulose microfibril suspension (3.3 wt %) was first mixed with a solution of gelatinized starch (3.1 wt %). The amount of each part was adjusted in order to obtain the required cellulose–starch content in the dry film. The cellulose filler content was varied from 0 to 50%. Glycerol was added as the plasticizer, and its content was expressed as a percentage of the total dry weight of the cellulose plus the starch. The amount of glycerol was varied between 0 and 30%. For example, a film referred to as 10% cellulose, 90% starch, and 30% glycerol, contains respectively 0.2, 1.8, and 0.6 g of each component, so the true cellulose content was only 8.3% of the material.

These suspensions were homogenized with a T25 Ultra-turax, but microbubbles were generated. The air was removed by pumping the suspension under a vacuum prior to casting in a Teflon mold and storing at 37°C.

### Transmission Electron Microscopy

Transmission electron microscopy (TEM) observations were achieved with a Philips CM200 operated at 80 kV. A drop of a dilute cellulose microfibrils suspension was deposited on carbon-coated grids and allowed to dry.

### Scanning Electron Microscopy

A scanning electron microscope (SEM) from Jeol (JSM-6100) was used to study the morphology of the raw materials. Small cubes were cut from potato tuber, fixed with glutaraldehyde and dried under critical point in a Polaron Critical Point Dryer operated with liquid CO<sub>2</sub>. The specimens were frozen under liquid nitrogen, then fractured, glued on a support, sputtered with a thin gold layer in a JEOL JFC-1100E ion sputter coater, and observed. SEM micrographs were obtained using 7 kV secondary electrons. SEM was also performed to investigate the morphology of the composite materials, following the same method for sample preparation.

### Tensile Tests

A model 4301 Instron Universal Testing Machine was used to analyze the nonlinear mechanical behavior in tensile mode, with a load cell of 100 N capacity. Test samples were thin rectangular strip (30 mm × 5 mm × 1 mm) and were cut from the films with a razor blade. The gap between pneumatic jaws at the start of each test was adjusted at ~ 20 mm. Tensile tests were performed at a strain rate  $\dot{\epsilon} = 8.3 \times 10^{-4} \text{ s}^{-1}$  (crosshead speed = 1 mm.min<sup>-1</sup>) and at 25°C. For each measurement, it was observed that the strain was uniform along the sample, until its break.

So, the strain can be determined by  $\epsilon = \ln(\lambda/\lambda_0)$ , where  $\lambda$  and  $\lambda_0$  are the length during the test and the length at zero time, respectively. The stress was calculated by  $\sigma = F/S$ , where  $F$  is the applied load and  $S$  is the cross-section.  $S$  was determined assuming that the total volume of the sample remained constant, so that  $S = S_0 \times \lambda_0/\lambda$ , where  $S_0$  is the initial cross-sectional area. Data allow the plotting of stress-versus-strain curves, and the tensile, or Young's, modulus ( $E$ ) was calculated from the initial slope in the vicinity of  $\sigma = \epsilon = 0$  ( $[d\sigma/d\epsilon]_{\epsilon \rightarrow 0}$ ). In order to have a more accurate comparison between the various materials, it was necessary to account for the film porosity, which can change in accordance with the film preparation. The corrected tensile modulus,  $E_{\text{corr}}$ , was calculated by taking into account the real cross-sectional area,  $S_{\text{corr}}$ , of the sample<sup>4</sup>

$$S_{\text{corr}} = \frac{M}{\rho \times L} \quad (1)$$

where  $M$  and  $L$  are the weight and the length, respectively, of the sample, and  $\rho$  is the density of

the material ( $\rho = 1.5 \text{ g/cm}^3$ ). The corrected tensile modulus ( $E_{\text{corr}}$ ) was then determined from the initial slope of the curve  $\sigma_{\text{corr}} = F/S_{\text{corr}} = f(\epsilon)$ . The values reported in this work result from the average of at least five measurements.

Starch as well as cellulose are strongly hydroscopic materials. It is therefore of interest to study the evolution of the mechanical properties with the moisture content. The moisture content of the composite films was achieved by conditioning the samples in dessicators at controlled humidities containing saturated salt solutions for at least 5 days until used. Three relative humidity (RH) conditions were used, namely, 25, 58, and 75%. The saturated salt solutions were potassium acetate (CH<sub>3</sub>COOK), sodium bromide (NaBr), and sodium chloride (NaCl), respectively. Therefore, the mechanical behavior of the cellulose microfibril/starch composite films was analyzed as a function of cellulose microfibril content, plasticizer content, and relative humidity.

### Water Uptake

The kinetics of water absorption was determined for all compositions. The specimens used were thin rectangular strips with dimensions of 10 mm × 10 mm × 1 mm. The films were therefore supposed to be thin enough for the molecular diffusion to be considered one dimensional. Samples were first dried overnight at 100°C. After weighting, they were conditioned at 25°C in a dessicator containing sodium sulfate in order to ensure an RH ratio of 95%. The conditioning of samples in a high moisture atmosphere was preferred to the classical technique of immersion in water because starch is very sensitive to liquid water and can partially dissolve after longtime exposure to water. They were then removed periodically, and the sample weight was measured using a four-digit balance. The water content or water uptake of the samples was calculated as follows:

$$\text{water uptake (\%)} = \frac{M_t - M_o}{M_o} \times 100 \quad (2)$$

where  $M_t$  and  $M_o$  are the weights at time  $t$  and before exposure to 95% RH, respectively.  $M_o$  corresponds therefore to the weight of dry solid, determined after drying overnight at 100°C. The mean moisture uptake of each sample was calculated at various conditioning times ( $t$ ). The mass of water sorbed at time  $t$  ( $M_t - M_o$ ) can be expressed as<sup>46</sup>

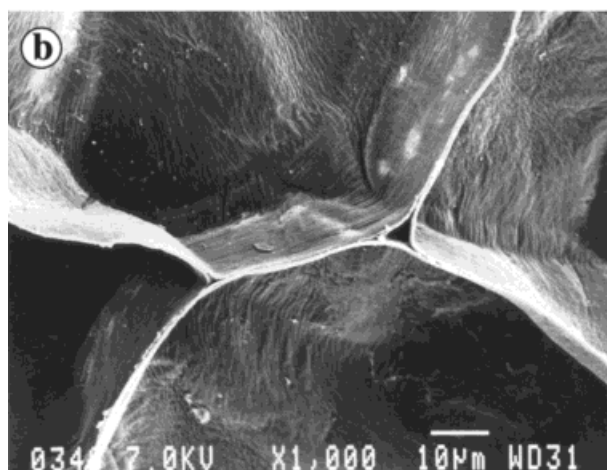
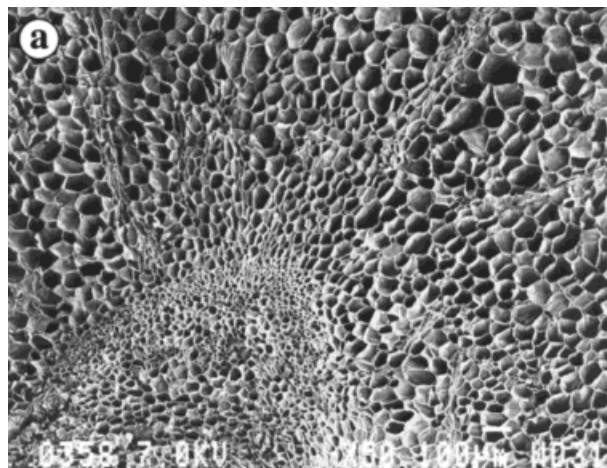


**Figure 2** Scanning electron micrograph of (a) parenchyma cells and vessels, and (b) parenchyma cells.

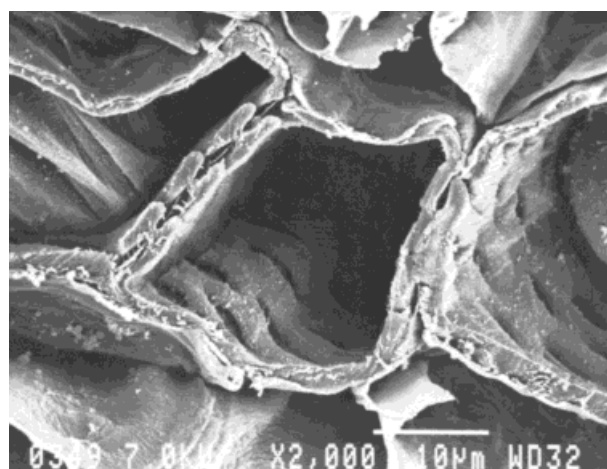


**Figure 3** Scanning electron micrograph of vessels showing reticulated vessels.

$$\frac{M_t - M_o}{M_\infty} = 1 - \sum_{n=0}^{\infty} \frac{8}{(2n+1)^2 \pi^2} \times \exp\left[\frac{-D(2n+1)^2 \pi^2 t}{4L^2}\right] \quad (3)$$

where,  $M_\infty$  is the mass sorbed at equilibrium,  $2L$  is the thickness of the polymer film, and  $D$  is the diffusion coefficient. At short times, eq. (3) can be written as

$$\frac{M_t - M_o}{M_\infty} = \frac{2}{L} \left(\frac{D}{\pi}\right)^{1/2} t^{1/2} \quad (4)$$

At  $(M_t - M_o)/M_\infty \leq 0.5$ , the error in using eq. (4) instead eq. (3) to determine the diffusion coefficient is on the order of 0.1%.<sup>47</sup>

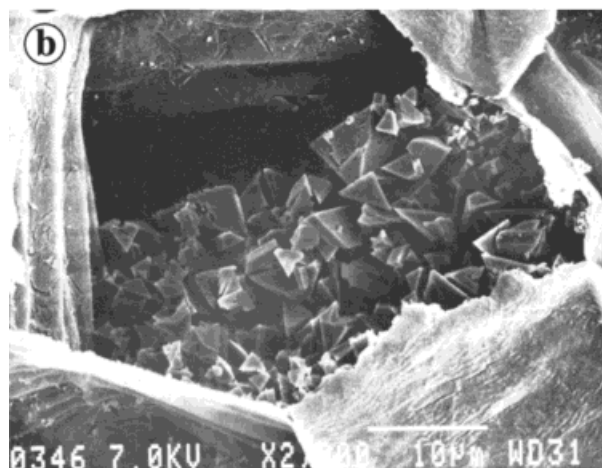
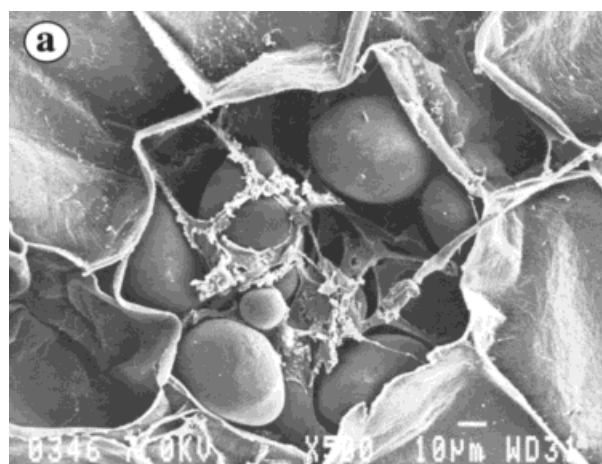


**Figure 4** Scanning electron micrograph showing (a) starch granules inside parenchyma cells, and (b) mineral crystals inside parenchyma cells.

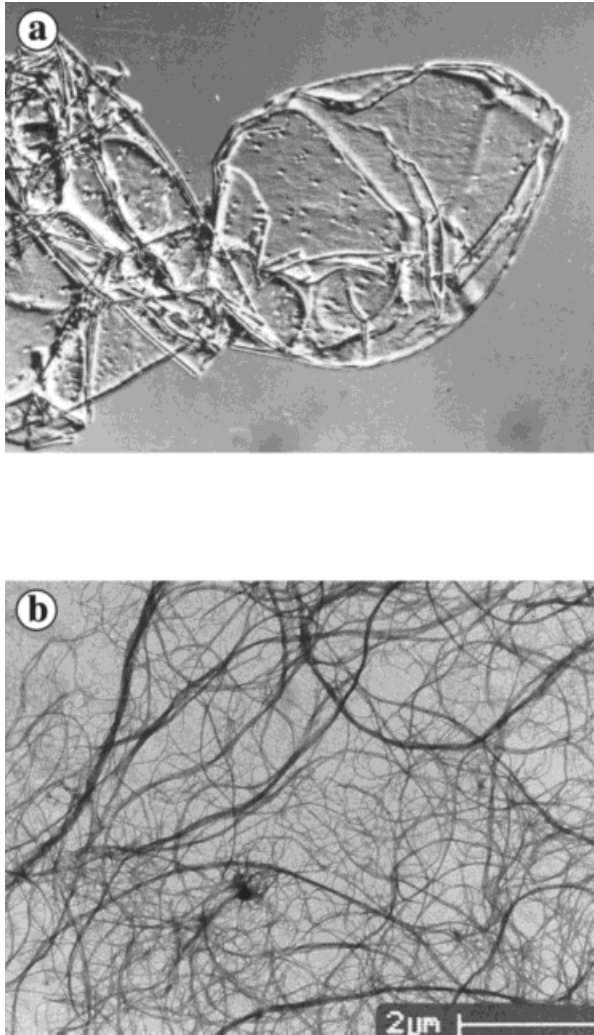


**Figure 5** (a) Optical micrograph in Nomarski contrast showing individualized potato cell wall. (b) Transmission electron micrograph showing individualized cellulose microfibrils after high-pressure mechanical treatment.

**RESULTS AND DISCUSSION**

**Morphology of the Potato Tuber**

The observation by SEM of transverse cross sections perpendicular to the long axis of the potato

tuber obtained after critical point drying displayed the presence of several kind of tissues: epidermic, parenchyma cells (Fig. 2), and reticulated vessels (Fig. 3). The external part of the tuber presented 4–6 rows of epidermic cells. It was noticeable that a relatively small amount of vessels and that most of the tuber consisted of parenchyma cells. The presence of residual starch granules inside the parenchyma cells was observed as beads with a diameter ranging between 10 and 100 μm [Fig. 4(a)]. Moreover, the presence was also observed of crystals inside some cells, corresponding most likely to calcium oxalate [Fig. 4(b)]. Potato tuber cells consist of thin cell walls, as shown in Figure 4(b). They are bound together by the middle lamella, which consists of pectic substances.

The alkali extraction (Fig. 1) with sodium hydroxide (NaOH) solution was expected to hydrolyze pectins by a β-elimination process and to solubilize them. This treatment induced the individualization of the different cells as flattened parenchyma cells with punctuation [Figure 5(a)], which can be observed by optical microscopy in Nomarski contrast. The chemical composition of potato tuber pulp after water washing and after two extractions with 2% NaOH is reported in Table I. The main difference in the data of Table I holds in the removal of arabino-galactane during alkaline extraction. Total hydrolysis showed that the crude pulp was composed of glucose, galactose, arabinose, xylose, and mannose in the molar proportions 49 : 32 : 11 : 3.6 : 0.2. After alkaline extraction, the molar proportions of the corresponding sugar were 92.9 : 1.3 : 1.5 : 3.5 : 1.0. Uronic acid determined by colorimetric method was estimated to be 10% in the crude pulp but only 2% after two 2% NaOH treatments.

After bleaching and freeze-drying, the cellulose pulp was suspended in distilled water and homogenized through a Manton Gaulin apparatus. The effect of the shearing treatment is well displayed in Figure 5(b), which shows transmission electron

**Table I Neutral Sugar Composition**

Compound	Sugars <sup>a</sup>						Total (%)
	% Glc	% Gal	% Man	% Xyl	% Ara	% Rha	
Potato tuber pellets	24.5	16	0.9	1.8	5.5	1.3	50
After 2% NaOH	72.5	0.9	0.7	2.7	1.2	0	78
After NaClO <sub>2</sub>	76	0.8	0.7	2.5	1.0	0	81

<sup>a</sup> Values are from gram quantities of anhydrosugar from 100 g of dry matter.

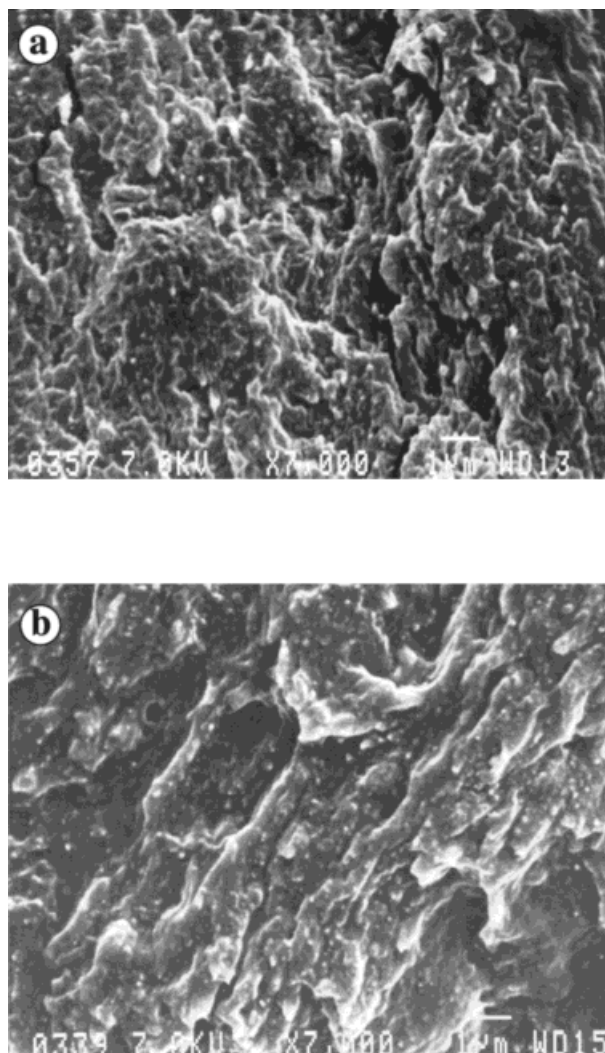


**Figure 6** Scanning electron micrographs of freshly fractured surface cellulose microfibrils/plasticized starch composite films: (a) 30% glycerol and 20% cellulose, and (b) 10% glycerol and 50% cellulose.

micrograph (TEM) of cellulose microfibril suspensions, with microfibrils well individualized or still associated together in bundles. Individual microfibrils are almost 5 nm in width, and the length is much higher, leading to a practically infinite aspect ratio of this filler.

SEM was also used to characterize the morphology of the cellulose microfibril-filled starch composites. Figure 6 shows the surface of a film, just after fracture, plasticized with 30% glycerol and filled with 20% cellulose microfibrils [Fig. 6(a), and plasticized with 10% glycerol and filled with 50% cellulose [Fig. 6(b)]. On these micrographs cellulose microfibril aggregates appear as white stains. It was observed that the dispersion of the filler within the matrix was homogeneous.

## Mechanical Behavior

**Starch–Glycerol Matrix.** The mechanical behavior of the unfilled starch–glycerol matrix was analyzed at room temperature as a function of glycerol content and relative humidity (RH). A typical stress-versus-strain curve is shown in Figure 7. The corrected tensile modulus,  $E_{\text{corr}}$ , of the starch–glycerol films, derived from the initial slope of the stress–strain plots, is plotted in Figures 8(a) and 8(b) versus glycerol content for samples conditioned at different RH levels and versus relative humidity for samples plasticized with different glycerol content, respectively. Solid lines serve to guide the eye. Because the starch film contains both amorphous and crystalline regions, the measured moduli are average values reflecting the contributions of each phase. Crystalline domains act as both filler and crosslinks on the mechanical properties, leading to an increase of the modulus. With increasing glycerol content, a decrease in the modulus is observed in Figure 8(a), regardless of the RH. This decrease is linear up to  $\sim 15\%$  glycerol. At higher glycerol content the modulus drop strongly increases. Moreover,  $E_{\text{corr}}$  is as low as the RH is high [Fig. 8(b)]. These two observations mean that both glycerol and water have a plasticizing effect on starch.

However, Figure 8(b) shows that the evolution of the  $E_{\text{corr}}$  versus moisture content is weak at a low glycerol content. At an intermediate glycerol content (10 and 15%), the material becomes more sensitive to the moisture content and displays a sharper decrease of modulus versus RH. At higher glycerol content, the modulus again de-

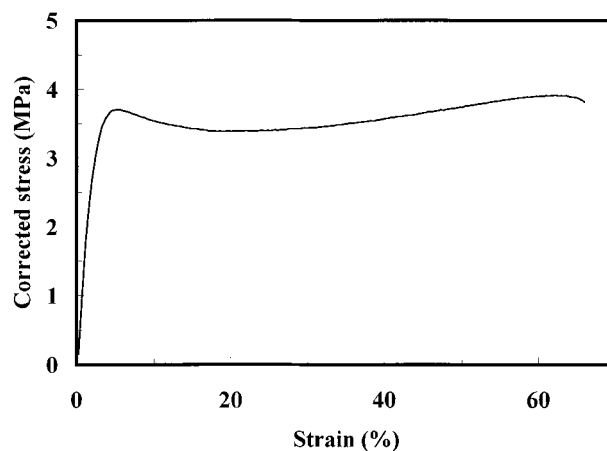


**Figure 7** Typical stress versus strain curve for a starch film plasticized with 20% glycerol at 25°C and 75% RH.  $\dot{\epsilon} = 8.3 \times 10^{-4} \text{ s}^{-1}$ .

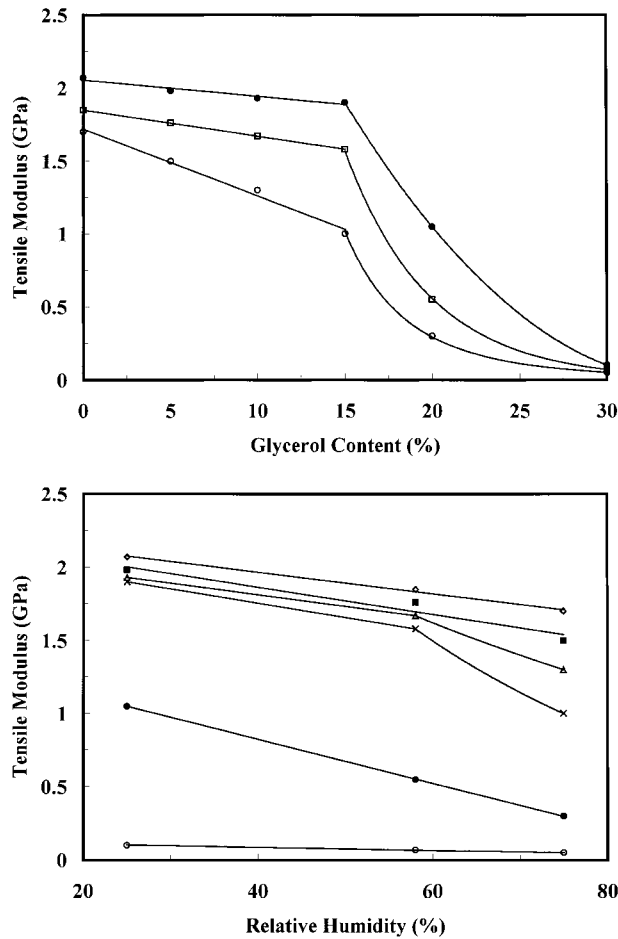


**Figure 8** Evolution of the corrected tensile modulus,  $E_{\text{corr}}$ , of the starch/glycerol films (a) conditioned at 25% (●), 58% (□), and 75% (○) RH, as a function of the glycerol content, and (b) plasticized with 0% (◇), 5% (■), 10% (△), 15% (×), 20% (●), and 30% (○) glycerol, as a function of the relative humidity. Solid lines serve to guide the eye.

increases slightly with moisture content. This abrupt change in mechanical properties for intermediate RH and glycerol content is due to the shift of the glass-rubber transition to a lower temperature. It is probably close to room temperature for 15% glycerol plasticized materials at high RH and for 20% glycerol plasticized starch at low RH. These values agree with the evolution reported for the glass-rubber transition temperature of potato starch films with glycerol content.<sup>48</sup>

*Cellulose Microfibril-Plasticized Starch Composites.* The corrected tensile modulus is plotted in Figure 9(a) versus cellulose content for three dif-

ferent glycerol contents (0, 15, and 30%) at 25% relative humidity (RH). It is worth noting that the cellulose microfibril content reported in this plot refers to the true cellulose content of the total system starch plus glycerol plus cellulose. It is shown that cellulose microfibrils appreciably reinforce the starch matrix, regardless of the glycerol content. The evolution of the tensile modulus as a function of the cellulose content is nearly linear. In addition, for a given filler loading, the higher modulus value is systematically observed for the less plasticized material. Similar behavior was observed at 58% and 75% RH [Figs. 9(b) and (c), respectively].

Concerning the starch-cellulose microfibril composites without any glycerol, the evolution of the modulus-versus-cellulose content is slightly affected by the RH ratio. It is clear that for unplasticized materials, the matrix is in the glassy state at room temperature, and then the absorption of water should be restricted. This effect can be correlated to the effectiveness of the reinforcing effect of the cellulose and to the existence of strong interactions between the filler and the matrix for glycerol-free samples.

When the starch matrix is plasticized with glycerol, a decrease in the slope of the plot of the modulus as a function of the cellulose content is observed when the RH ratio increases. These composite materials are therefore strongly sensitive to the moisture content. This phenomenon is ascribed to the starch being in the rubbery state at room temperature (for 30% glycerol), when the matrix should be able to absorb more water. The reinforcing effect of the cellulose filler is therefore strongly diminished. The material can be visualized as a microfibril network surrounded by the starch matrix, similar to what was observed by Dufresne et al.<sup>41</sup> for sugar beet cellulose microfibrils-pectin systems. Because starch is more hydrophilic than cellulose, in moist conditions it absorbs most of the water and is then plasticized. The cellulosic network is therefore surrounded by a soft phase. The interactions between the filler and the matrix are strongly reduced, and the modulus remains practically constant, whatever the composition may be.

The effectiveness of the reinforcing effect of the starch matrix by the cellulose can be well displayed by plotting the relative modulus versus cellulose content (Fig. 10). It is clear from these plots that the reinforcing effect is rather low for low glycerol content compositions. When the glycerol content increases, the  $T_g$  of the matrix de-



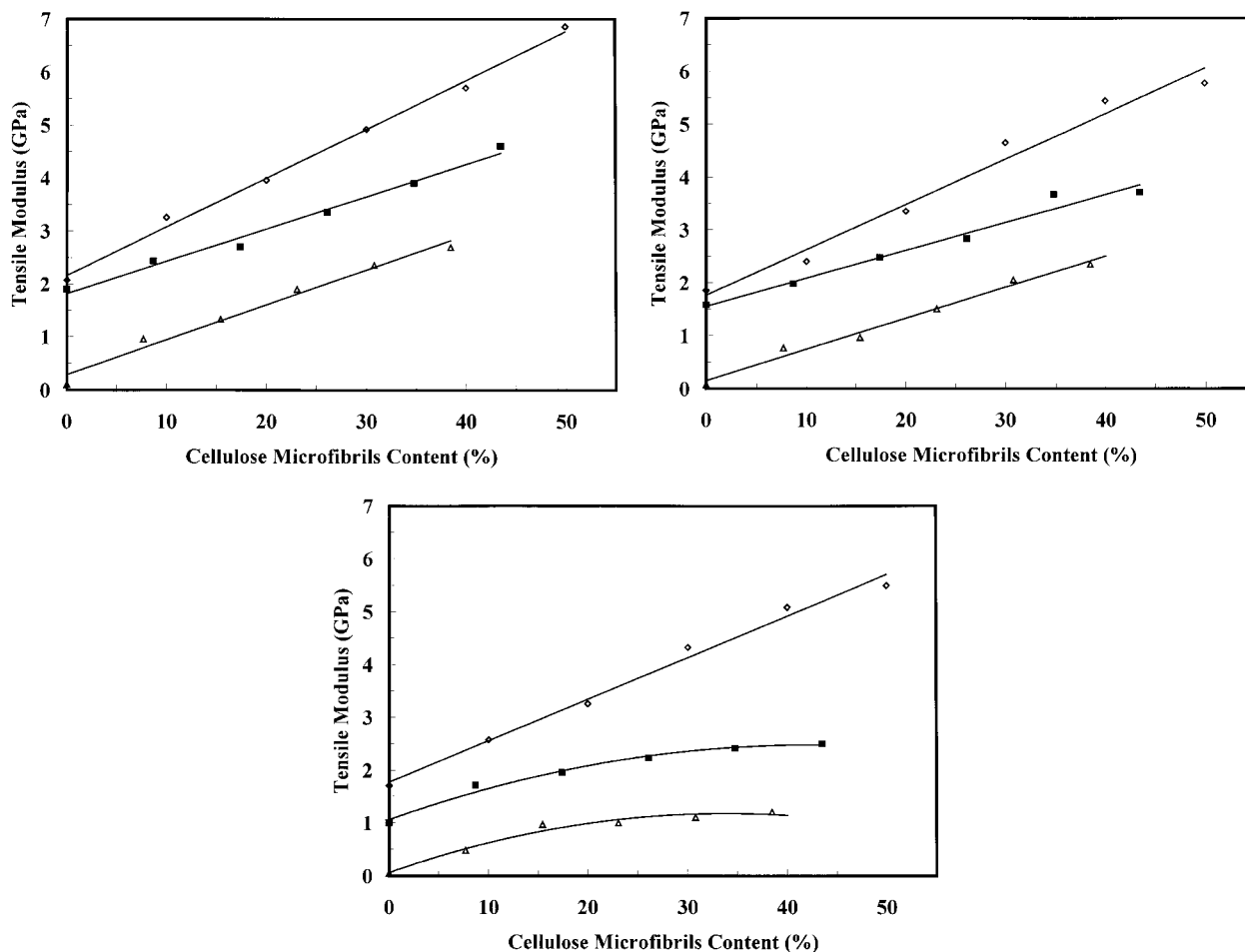


**Figure 9** Evolution of the corrected tensile modulus,  $E_{corr}$ , of the starch/glycerol films plasticized with 0% ( $\diamond$ ), 15% ( $\blacksquare$ ), and 30% ( $\triangle$ ) glycerol conditioned at (a) 25%, (b) 58%, and (c) 75% RH, as a function of the cellulose microfibrils content. Solid lines serve to guide the eye.

creases down to temperatures lower than room temperature, and the effect of adding filler becomes more significant. A simple mixing rule accounts for this phenomenon. At a high RH, this strong reinforcing effect shades off progressively when adding more microfibrils.

### Water Sorption Behavior

In sorption kinetics experiments, the mass of sorbed penetrant is measured as a function of time. The change in weight during conditioning at 95% RH is plotted against time in Figures 11(a) and 11(b) for films plasticized with 0% and 30% glycerol, respectively. These swelling data are the results of several trials, and the measurement reliability was very good. We ascertained that each composition absorbed water during the ex-

periment but behaved differently. Two well-separated zones are displayed in Figure 11. At lower times (zone I:  $t < 100$  h), the kinetics of absorption are fast, while the longtime kinetics of absorption are slow and lead to a plateau (zone II). In zone I the water uptake for a given time is always as low as the cellulose microfibril content is high. In zone II the water uptake reaches a plateau whose value is always as low as the cellulose content is high. It corresponds to the weight percentage increase at equilibrium or the water uptake at equilibrium.

The maximum relative water uptake, or water uptake at equilibrium, is plotted in Figure 12 versus the composition for unplasticized and for 30% glycerol plasticized starch-based composites. It was found that unfilled and unplasticized

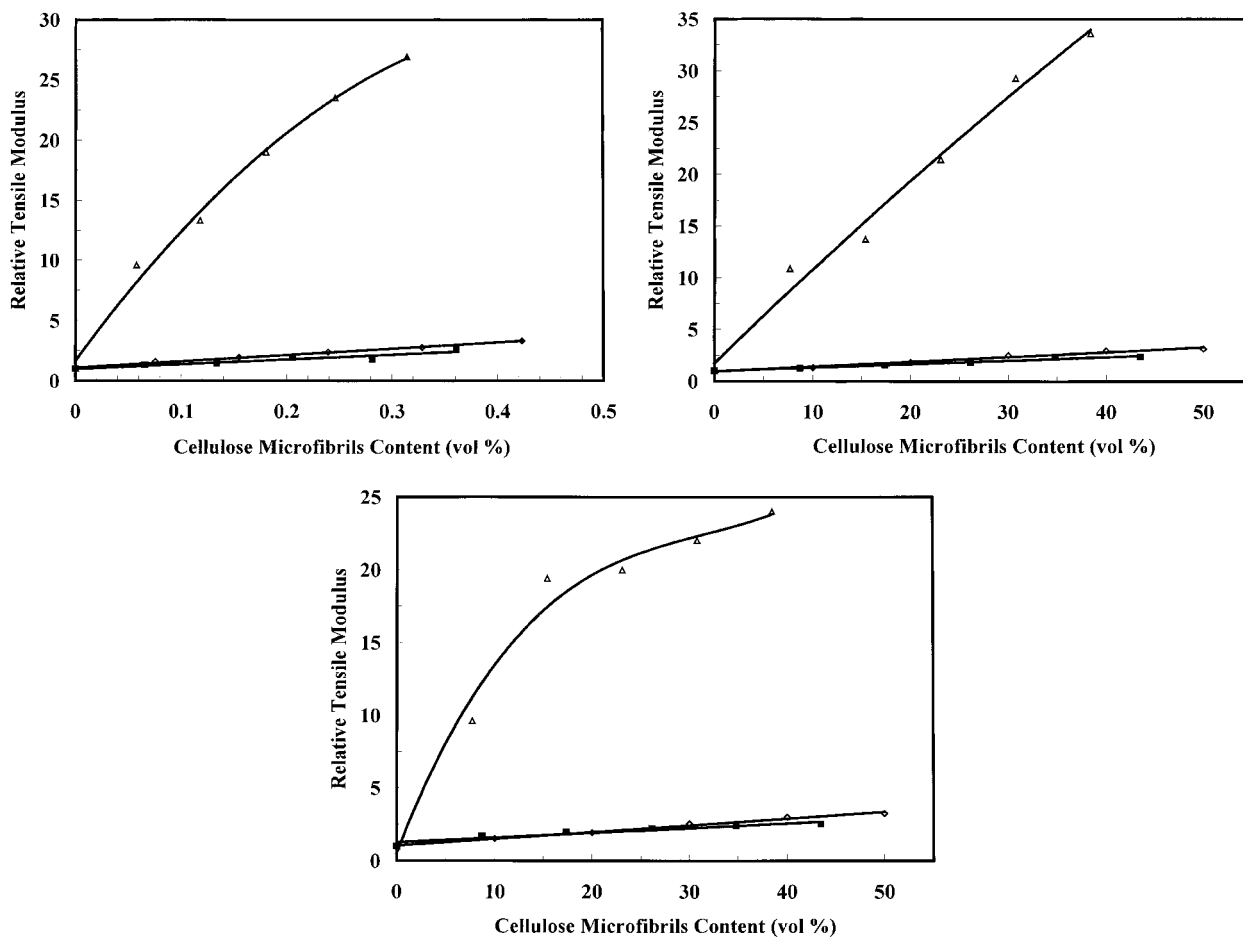


**Figure 10** Relative tensile modulus of the starch/glycerol films plasticized with 0% ( $\diamond$ ), 15% ( $\blacksquare$ ), and 30% ( $\triangle$ ) glycerol conditioned at (a) 25%, (b) 58%, and (c) 75% RH, as a function of the cellulose microfibrils content. Solid lines serve to guide the eye.

starch absorbs around 30% water. It corresponds to  $\sim 1.31$  g of water per gram of starch. This value is very close to that reported for microcrystalline starch ( $\sim 1.17$  g of water per gram of starch).<sup>21</sup> The difference between these two values occurs from the semicrystalline starch being able to absorb a higher water level than starch microcrystals. A starch matrix prepared without glycerol absorb two times less water than strongly plasticized materials. Indeed, the water uptake at equilibrium of the 30% glycerol plasticized film is around 58%. It corresponds to  $\sim 1.6$  g of water per gram of plasticized starch.

This increase in maximum water uptake is ascribed to the more hydrophilic nature of glycerol with respect to starch. Moreover, it is clear from Figure 12 that water uptake decreases with increasing cellulose content, regardless of the plasti-

cization state. For instance, the maximum relative water uptake of the unplasticized film is around 30% for the unfilled material, while it is only 18% for the starch matrix filled with 40% cellulose microfibrils. For the 30% glycerol plasticized film, it is around 58% and 30% for the unfilled and the 40% cellulose-filled starch matrices, respectively. Therefore, the presence of cellulose microfibrils within the starch material decreases water sensitivity. In addition, water uptake at equilibrium decreases roughly linearly versus cellulose microfibril content, and the full lines in Figure 12 correspond to the best linear fits, whose equations are

$$\frac{M_t - M_o}{M_o} \Big|_{t \rightarrow \infty} = 28.92 - 0.266 w_f$$

for the unplasticized starch

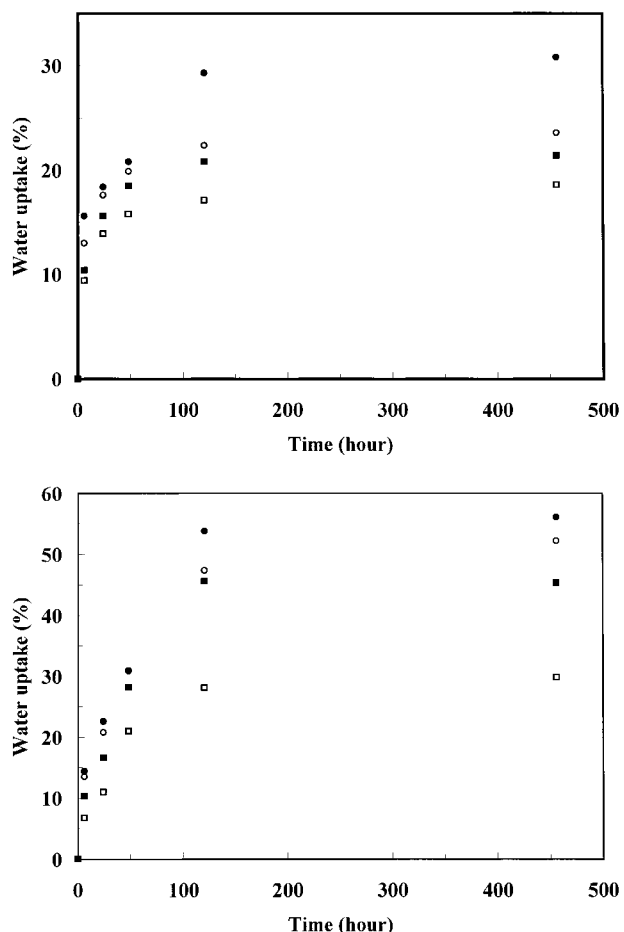


**Figure 11** Water uptake during conditioning at 95% RH versus time for (a) unplastized and (b) 30% glycerol plastized starch/glycerol films filled with 0 (●), 10 (○), 30 (■), and 40% (□) of cellulose microfibrils.

$$\frac{M_t - M_o}{M_o} \Big|_{t \rightarrow \infty} = 57.75 - 0.773 w_f$$

for the 30% plastized starch (5)

where  $w_f$  is the cellulose microfibril weight fraction. It was observed that the effect of the cellulose microfibril content on water sensitivity is more drastic for the plastized system.

The water diffusivity or diffusion coefficient,  $D$ , of water in the starch-based material was estimated using eq. (4). The plots of  $(M_t - M_o)/M_\infty$  as a function of  $(t/L^2)^{1/2}$  were performed for all the compositions and for  $(M_t - M_o)/M_\infty \leq 0.5$ . It was observed that the behavior was Fickian. The diffusion coefficients calculated from the slope of these plots are reported in Table II. Figure 13 shows the evolution of the diffusion coefficient versus sample composition.

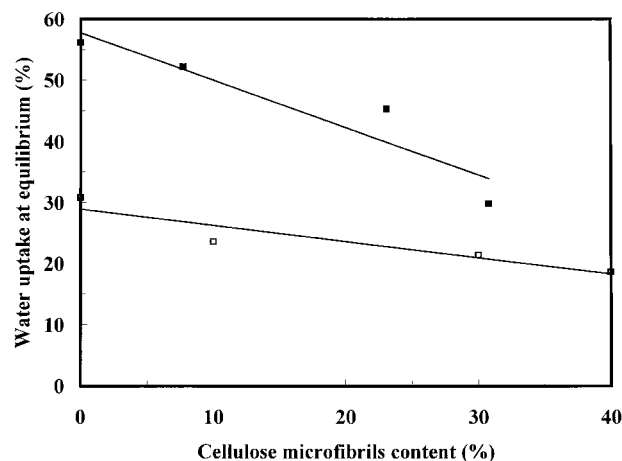


**Figure 12** Water uptake at equilibrium versus cellulose microfibrils content for 0% (□) and 30% (■) glycerol plastized starch films.

By comparing the  $D$  values of unfilled plastized and unplastized starch films, it was observed that the diffusion coefficient of water is higher for the unplastized system. This is an unexpected result. Indeed, the glass transition temperature of starch decreases as the glycerol content increases. This lowering of  $T_g$  reflects enhanced chain mobility at room temperature and should result in an increase of diffusion coefficient with glycerol content. However, the addition of dextrin, sucrose, and glucose to starch to simulate the effect of low molecular weight carbohydrates on the diffusion of water was found to reduce the moisture diffusivity of granular starches in proportion to their percentage.<sup>49</sup> Glycerol is a low molecular weight molecule and brings a similar effect. Therefore, despite the water uptake being higher in the plastized system,

**Table II** Water Diffusion Coefficients  $D$  in Starch-Cellulose Microfibril Composites Conditioned at 95 RH

Cellulose Content (%)	$D$ (cm <sup>2</sup> /s)	
	0% Glycerol	30% Glycerol
0	$5.04 \times 10^{-10}$	$1.10 \times 10^{-10}$
10 [7.69] <sup>a</sup>	$3.53 \times 10^{-10}$	$8.39 \times 10^{-11}$
30 [23.08] <sup>a</sup>	$1.65 \times 10^{-10}$	$5.25 \times 10^{-11}$
40 [30.77] <sup>a</sup>	$1.72 \times 10^{-10}$	$2.08 \times 10^{-11}$

<sup>a</sup> The amount of cellulose in the plastized systems refers to the starch + cellulose content. Data in square brackets refer to the true cellulose content of the total system starch + glycerol + cellulose.

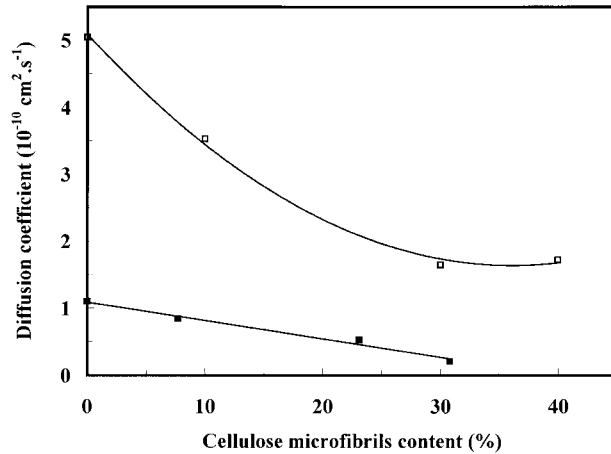


**Figure 13** Evolution of the diffusion coefficient versus cellulose microfibrils content for 0% (□) and 30% (■) glycerol plasticized starch films.

the kinetic of water absorption, displayed through the water diffusion coefficient, is hindered by glycerol. It is about five times lower for the 30% glycerol plasticized starch compared to the unplasticized one. These diffusion coefficients of water in starch are much lower than those reported in the literature, as it was measured using weight loss<sup>49–51</sup> and NMR techniques.<sup>52,53</sup> Both methods yield  $D$  values on the order of  $10^{-6}$  cm<sup>2</sup>/s. However, the measurement technique used in the present work is quite different because samples were conditioned in a high-moisture atmosphere (RH = 95%), and the kinetic of water transport is expected to be much lower than during immersion in liquid water.

The diffusion coefficient of water in starch is always lower as the cellulose microfibril content is high, regardless of the plasticization state of the matrix. For unplasticized starch, it decreases from  $5 \times 10^{-10}$  cm<sup>2</sup> s<sup>-1</sup> to  $1.7 \times 10^{-10}$  cm<sup>2</sup> s<sup>-1</sup> as the cellulose microfibrils content increases from 0 to 30% wt %. It seems to stabilize at higher filler content. For the plasticized system,  $D$  decreases linearly over the whole explored filler content range with a slope around  $-2.7 \times 10^{-10}$  cm<sup>2</sup> s<sup>-1</sup>. As reported for the unfilled material, the diffusion coefficient is systematically higher in the unplasticized starch than in the plasticized material, despite the water uptake at equilibrium being lower in the former system.

Therefore, the three-dimensional intertwined cellulose microfibril network observed in the filler suspension [Fig. 5(b)] is probably preserved when mixed with gelatinized starch. The film processing by water evaporation allows stabilization of

this structure and reinforces it by the establishment of strong hydrogen bonds between cellulose microfibrils during the evaporation step. This phenomenon is similar to the percolation of cellulose fibers in paper making.<sup>54,55</sup> Indeed, it is well established that the high mechanical properties of a paper sheet result from the hydrogen-bonding forces that hold the percolating network of the fibers. In our systems cellulose microfibrils act as a close network within the matrix and prevent the swelling of the starch material when exposed to water or moist atmosphere. In addition, favorable interactions probably exist between starch and cellulose that contribute to this phenomenon. Adding cellulose microfibrils to the starchy matrix results in a decrease of both water uptake at equilibrium and the water diffusion coefficient.

## CONCLUSIONS

Potato tuber cells were individualized under alkaline conditions and homogenized under shearing to produce cellulose microfibril suspensions. The resulting suspension was used as a cheap and environmentally friendly filler to process composite materials, causing a high level of dispersion, with gelatinized potato starch as the matrix and glycerol as a plasticizer. The mechanical properties at room temperature of these systems were investigated using a tensile test. It was shown that both glycerol and water plasticize the starch matrix. The highest mechanical properties were obtained with an unplasticized starch matrix in a dry atmosphere. The reinforcing effect was more significant in plasticized starch due to the decrease of  $T_g$  of the matrix down to temperatures lower than room temperature. However, the mechanical properties of highly plasticized materials were found to depend strongly on relative humidity (RH) conditions. Water absorption behavior was also characterized on materials conditioned at 95% RH. It was found that water sensitivity linearly decreases with the cellulose microfibril content. This result means new applications for the starch material can be envisioned. In addition, it is worth noting that any agricultural residue can be used as a source for processing cellulose microfibrils.

The authors gratefully acknowledge Avebe Company for supplying dry potato pulp, Mr. X. Martin for his help in preparing composite films, and Dr. H. Chanzy for his help in TEM.

## REFERENCES

1. Stepto, R. F.; Tomka, I. *Chimia* 1987, 41, 76.
2. Bastioli, C.; Belloti, V.; Del Giudice, L.; Lambi, R. *Eur. Pat. Appl. EP* 400,532 (1990).
3. Roper, H.; Koch, H. *Starch* 1990, 42, 123.
4. Tomka, I. *PCT Pat. Appl. WO* 90/05161, 1990.
5. Chinnaswamy, R.; Hanna, M. A. *Starch* 1991, 43, 396.
6. Lai, L. S.; Kokini, J. L. *Biotechnol Prog* 1991, 7, 251.
7. Wiedmann, W.; Strobel, E. *Starch* 1991, 43, 138.
8. Gonsalves, K. E.; Patel, S. J.; Chen, X. *New Polym Mater* 1990, 2, 175.
9. Goheen, S. M.; Wool, R. P. *J Appl Polym Sci* 1991, 42, 2691.
10. Imam, S. H.; Gould, J. M.; Kinney, M. P.; Ramsey, A.; Tosteson, T. R. *Cur Microbiol* 1992, 25, 1.
11. Orford, P. D.; Parker, R.; Ring, S. G.; Smith, A. C. *Int J Biol Macromol* 1989, 11, 91.
12. Russel, P. L. *J Cereal Sci* 1987, 6, 133.
13. Shogren, R. L. *Carbohydr Polym* 1992, 19, 83.
14. Poutanen, K.; Forssell, P. *TRIP* 1996, 4, 128.
15. van Soest, J. J. G.; Benes, K.; de Wit, D.; Vliegthart, J. F. G. *Polymer* 1996, 37, 3543.
16. van Soest, J. J. G.; de Wit, D.; Vliegthart, J. F. G. *J Appl Polym Sci* 1996, 61, 1927.
17. Lourdin, D.; Bizot, H.; Colonna, P. *J Appl Polym Sci* 1997, 64, 1047.
18. Westhoff, R. P.; Otey, F. H.; Mehlretter, C. L.; Russell, C. R. *Ind Eng Chem Prod Res Dev* 1974, 13, 123.
19. Griffin, G. J. L. *Brit. Pat.* 1,485,833 (1972).
20. Dufresne, A.; Cavallé, J. Y.; Helbert, W. *Macromolecules* 1996, 29, 7624.
21. Dufresne, A.; Cavallé, J. Y. *J Polym Sci Polym Phys* 1998, 36, 2211.
22. Seymour, R. B. *Popular Plastics* 1978, 11, 27.
23. Lightsey, G. R. In *Polymer Application of Renewable Resource Materials*; Carraher Jr., C. E.; Sperling, L. H. Eds. Plenum Press: New York, 1983; Vol. 93.
24. Joseph, K.; Thomas, S.; Pavithran, C.; Brahmakumar, M.; *J Appl Polym Sci* 1993, 47, 1731.
25. Varghese, S.; Kuriakose, B.; Thomas, S. *J Appl Polym Sci* 1994, 53, 1051.
26. Felix, J. M.; Gatenholm, P. *J Mater Sci* 1994, 29, 3043.
27. Jain, S.; Kumar, R.; Jindal, U. C. *J Mater Sci* 1992, 27, 4598.
28. Basu, D.; Banerjee, A. N.; Misra, A. *J Appl Polym Sci* 1992, 46, 1999.
29. Avella, M.; Martuscelli, E.; Pascucci, B.; Raimo, M.; Foher, B.; Marzetti, A. *J Appl Polym Sci* 1993, 49, 2091.
30. Sanadi, A. R.; Rowell, R. M.; Caulfield, D. F. *Polymer News* 1996, 20, 7.
31. Raj, R. G.; Kokta, B. V.; Maldas, D.; Daneault, C. *Polym Compos* 1988, 9, 404.
32. Maldas, D.; Kokta, B. V.; Daneault, C. *J Appl Polym Sci* 1989, 38, 413.
33. Favier, V.; Canova, G. R.; Cavallé, J. Y.; Chanzy, H.; Dufresne, A.; Gauthier, C. *Polym Adv Tech* 1995, 6, 351.
34. Helbert, W.; Cavallé, J. Y.; Dufresne, A. *Polym Compos* 1996, 17, 604.
35. Dufresne, A.; Cavallé, J. Y.; Helbert, W. *Polym Compos* 1997, 18, 198.
36. Dufresne, A. *Recent Res Devel in Macromol Res* 1998, 3, 455.
37. Dinand, E.; Chanzy, H.; Vignon, M. R.; Maureaux, A.; Vincent, I. *French Pat.* 2,730,252 (1995).
38. Dinand, E.; Chanzy, H.; Vignon, M. R. *Cellulose* 1996, 3, 183.
39. Dinand, E.; Chanzy, H.; Vignon, M. R. *Food Hydrocolloids* 1999, 13, 275.
40. Dufresne, A.; Vignon, M. R. *Macromolecules* 1998, 31, 2693.
41. Dufresne, A.; Cavallé, J. Y.; Vignon, M. R. *J Appl Polym Sci* 1997, 64, 1185.
42. Blumenkrantz, P. N.; Asboe-Hansen, G. *Anal Biochem* 1973, 54, 484.
43. Selvendran, R. R.; March, J. F.; Rings, S. G. *Anal Biochem* 1979, 96, 282.
44. Wise, L. E. M.; Murphy, M.; d'Addiecco, A. A. *Paper Trade J* 1946, 122, 35.
45. Turbak, A. F.; Snyder, F. W.; Sandberg, K. R. *U.S. Pat.* 4,374,702 (1983).
46. Comyn, J. In *Polymer Permeability*; Comyn, J. Ed., Elsevier Applied Science: New York, 1985.
47. Vergnaud, J. M. In *Liquid Transport Processes in Polymeric Materials: Modeling and Industrial Applications*; Prentice-Hall: Englewood Cliffs, 1991.
48. Lourdin, D.; Bizot, H.; Colonna, P. *J Appl Polym Sci* 1997, 63, 1047.
49. Marousis, S. N.; Karathanos, V. T.; Saravacos, G. D. *J Food Sci* 1989, 54, 1496.
50. Karathanos, V. T.; Villalobos, G.; Saravacos, G. D. *J Food Sci* 1990, 55, 218.
51. Marousis, S. N.; Karathanos, V. T.; Saravacos, G. D. *J Food Process Preservation* 1991, 15, 183.
52. Callaghan, P. T.; Jolley, K. W.; Lelievre, J. *Biophys J* 1979, 28, 133.
53. Umbach, S. L.; Davis, E. A.; Gordon, J.; Callaghan, P. T. *Cereal Chemistry* 1992, 69, 637.
54. Batten Jr., G. L.; Nissan, A. H. *TAPPI* 1987, 70, 119.
55. Nissan, A. H.; Batten Jr., G. L. *TAPPI* 1987, 70, 128.